

Fast imaging polarimeter for magneto-optical investigations

Rinke J. Wijngaarden,^{a)} K. Heeck, M. Welling, R. Limburg, and M. Pannetier
*Faculty of Sciences, Division of Physics and Astronomy, Vrije Universiteit, De Boelelaan 1081,
 1081 HV Amsterdam, The Netherlands*

K. van Zetten, V. L. G. Roorda, and A. R. Voorwinden
ARVOO Engineering BV, P.O. Box 439, 3440 AK Woerden, The Netherlands

(Received 3 October 2000; accepted for publication 27 February 2001)

A new imaging polarimeter for magneto-optical investigations is described. Improvements over conventional magneto-optics are: it (i) is insensitive to uneven illumination, (ii) determines also the sign of the magnetic field, and (iii) has significantly improved sensitivity at small magnetic fields. The typical root-mean-square (rms) noise level is $0.7 \text{ mT Hz}^{-1/2}$ for a single pixel, corresponding to a polarization rotation of $0.03 \text{ deg Hz}^{-1/2}$. With limited temporal and spatial averaging, the rms error in magnetization profiles can be reduced to $<10 \mu\text{T}$, corresponding to $4 \times 10^{-4} \text{ deg}$. Time resolution is 12 frames per second. Demonstration of the performance of the polarimeter is given for measurements of the local field above superconductors and for measurements of the rotation angle of sugar dissolved in water. © 2001 American Institute of Physics. [DOI: 10.1063/1.1368855]

I. INTRODUCTION AND METHOD

Imaging polarimetry is used in a wide range of fields both in remote sensing (such as astrophysics¹ and solar physics²) and in laboratory measurements (e.g., condensed matter physics³). In this article, we present a new imaging polarimeter with enhanced properties and demonstrate its performance in measurements on sugar dissolved in water and in magneto-optical imaging of the dynamics of vortex matter in superconductors.

Conventionally, the local magnetic-field map due to supercurrents or vortices in a superconductor is visualized using an indicator layer with high Verdet constant V and a polarization microscope.³ The indicator layer of thickness l (typically, $0.5\text{--}2.0 \mu\text{m}$) is in direct contact with the superconductor and rotates the polarization vector of the incident linear polarized light over an angle ϕ proportional to the local magnetic field B according to $\phi = VlB$. Between the crossed polarizers of a polarization microscope the square of the local magnetic field is thus imaged as an intensity map. Unfortunately, this type of setup has three main disadvantages: (i) the sign of the rotation angle of the polarization vector and, hence, of the magnetic field, cannot be determined; (ii) the setup is very insensitive for small magnetic fields/angles; and (iii) the measured intensity distribution is strongly influenced by the inhomogeneous illumination.

In this article, we report on a new method which circumvents all these problems.

The transmitted intensity in a polarization microscope with a sample placed between the polarizer and analyzer is

$$I = L \sin^2(\alpha + \phi) \approx L(\alpha + \phi)^2,$$

where ϕ is the rotation angle due to the sample, $(90^\circ - \alpha)$ is the angle between the polarizer and analyzer, and L is the incident intensity. For $\alpha=0$, i.e., with perfectly crossed po-

larizer and analyzer, the intensity depends quadratically on ϕ for small ϕ . This results in poor sensitivity close to $\phi=0$ while the method gives no information on the sign of ϕ . To increase the sensitivity close to $\phi=0$, sometimes α is set to a small nonzero value. We expand this idea by modulating the incident polarization direction. Since the sinusoidal modulation used for nonimaging Kerr measurements has the disadvantage that a lot of processing is needed to determine ϕ and also has a response time lower than the modulation frequency (which due to Nyquist's⁴ sampling theorem must be much lower than the image acquisition rate), we use a modulation with only three fixed values of α . This is justified since, even if we take into account that there may be an intensity offset K (due to camera noise, readout offset, or stray light) resulting in a measured intensity

$$I \approx K + L(\alpha + \phi)^2, \quad (1)$$

only three measurements suffice to determine K , L , and ϕ . We choose to measure at $\alpha = -\alpha_0$, 0 , and $+\alpha_0$, where α_0 is typically of the order of the maximum rotation due to the sample (a few degrees); the corresponding intensities are denoted by I_- , I_0 , and I_+ . It is easily verified that L and ϕ can be found from such a measurement using

$$L = \frac{I_- - 2I_0 + I_+}{2\alpha^2} \quad (2)$$

and

$$\phi = \frac{(I_+ - I_-)}{4\alpha L} \quad (3)$$

(of course K can also be determined, but is not of interest here). This algorithm is applied to each pixel separately. Since L is the measured illumination intensity, which is constant in time, it can be determined essentially noise-free by averaging over many images. The time resolution of the ex-

^{a)}Electronic mail: rw@nat.vu.nl

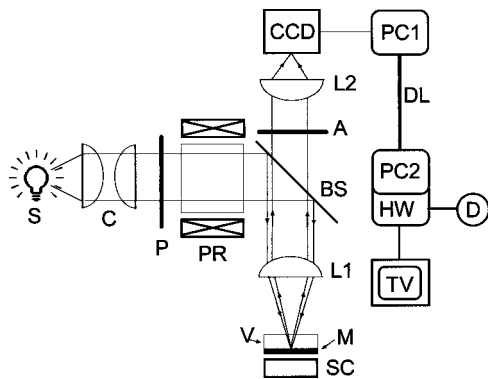


FIG. 1. Schematic diagram of the setup. Light from a light source (S) is collimated by a condenser (C) before passing through a polarizer and polarization rotator (PR) using the Faraday effect in a rod of special glass. The linearly polarized light then hits the beamsplitter (BS) and is focused by the lens (L1) onto the sample assembly, where the light passes through a layer (V) with a high Verdet constant, before being reflected by a mirror (M) in close contact with the (e.g., superconducting) sample (SC). The light exiting the sample passes through the lens (L1), the beamsplitter (BS), and an analyzer (A) and is focused by the lens (L2), which projects an image of the sample on the CCD chip of the video camera (CCD). Depending on the type of camera, its output is either coupled directly to PC2 or through a camera controlling PC (PC1) and a high-speed digital link (DL). (PC2) is a PC hosting special hardware (HW), incorporating 22 digital signal processors, which carries out the calculation defined by Eqs. (2) and (3) on each pixel in the image at a rate of 25 input images per second. The output of the calculation is shown on a TV monitor (TV) and stored on a disk (D).

periment is not influenced by averaging L , because the time-dependent information in ϕ is only propagated by the numerator of Eq. (3).

II. EXPERIMENTAL SETUP

To experimentally determine ϕ , we have built dedicated hardware that performs the calculation of Eqs. (2) and (3) for each pixel in a video stream at an input frame rate of 25 images per second. In the experimental setup, see Fig. 1, the incoming light is linearly polarized by fixed polarizer (P). The angle α is set by passing the linearly polarized light through a polarization rotator (PR) before entering the sample. A beamsplitter (BS) then projects the light through the lens (L1) onto the sample assembly, where the light passes through a layer (V) with a high Verdet constant, before being reflected by a mirror (M) in close contact with the sample (SC). The light exiting the sample passes through lens (L1), the beamsplitter and an analyzer (A) and is focused by the lens (L2), which projects an image of the sample on the charge-coupled-device (CCD) chip of the video camera (CCD), which registers an intensity image according to Eq. (1). The polarization rotator is a 150-mm-long rod of SF 59 glass,⁵ which has a large Verdet constant, in a copper coil capable of generating 100 mT with a field inhomogeneity inside the glass of $<1\%$ and specially developed electronics, which switches the magnetic field in 1 ms during the video blank time. The copper coil is water cooled to prevent temperature-induced strain in the glass rod. Depending on the experiment, a Princeton Instruments ST-133 MicroMax photon-counting camera or a simple low-light-level surveillance b/w CCD camera is used. We found that due to

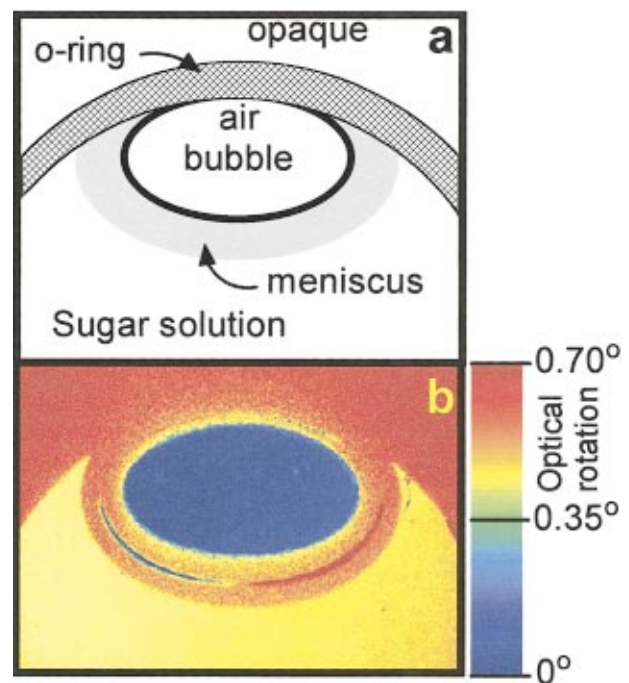


FIG. 2. (Color) Test sample using sugar dissolved in water and an air bubble in an O-ring. The experimental situation is schematically indicated in (a). Due to the meniscus of the water (shown as the gray region), no light is transmitted around the air bubble. Light transmission outside the O-ring is blocked to prevent overexposure. The color-coded polarization-rotation image is shown in (b). The sugar solution rotates the polarization vector by 0.51° (yellow), while there is no rotation (blue) by the air bubble. Note the clear contrast between the polarization inactive air and the sugar solution.

the high efficiency of this new method, the range of experiments where the simple camera can be used is extended.

The video signal of the surveillance camera is connected directly to the input of the image-processing PC (PC2), while the ST-133 camera is connected to a control PC (PC1), from which a high-speed digital link (DL) is connected to the image-processing PC (PC2). In this PC, specially designed hardware (HW), incorporating a total of 22 Analog Devices 21062 floating point Sharc Digital Signal Processors (DSPs), carries out the calculation defined by Eqs. (2) and (3). The division in Eq. (3), however, is not implemented, since a division takes much more time than a multiplication. Instead, we choose to combine the division and the averaging of L by the iterative algorithm

$$M_i = M_{i-1} [1 + k - M_{i-1} (I_- + I_+ - 2I_0)], \quad (4)$$

which yields $M = L^{-1}$ so that in Eq. (3) only a simple multiplication is needed. The inverse time constant is given by k . The apparatus can process in sustained mode up to 25 input images per second with image format of 782×582 pixels and 16 bits per pixel. Processing is done in floating point and output is written as 16 bit integers to a 36 Gbyte hard disk at a maximum sustained rate of 12 Mbyte/s.

III. RESULTS

To demonstrate the capability of this polarimeter, we present some experimental results. In Fig. 2, a test measurement is shown on sugar dissolved in water plus an air bubble inside an O-ring. The sugar solution rotates the polarization vector by 0.51° . The curved meniscus and the O-ring effec-

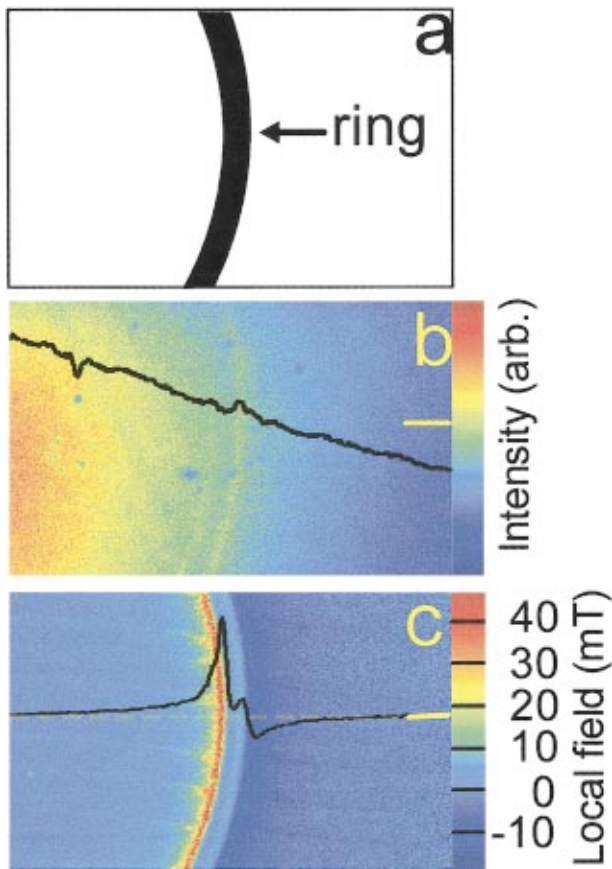


FIG. 3. (Color) Magneto-optical measurement of the perpendicular component of the magnetic field due to superconducting currents in a 100-nm-thick $\text{YBa}_2\text{Cu}_3\text{O}_7$ superconducting ring of 3 mm outer diameter and 125 μm width. In (a) the region of the ring under study is shown schematically. (b) is a conventional 50 ms exposure magneto-optic image with poor homogeneity of the illumination, and (c) is the ϕ output of the new apparatus under the same conditions. Note that 1 mT corresponds to 0.04° polarization rotation. Profiles taken at the height indicated by the yellow lines are shown in black. The zero-field level is indicated by the horizontal yellow dashed line.

tively block transmission and appear red. Note the very nice contrast between the air (which does not rotate the polarization vector) and the sugar water: the noise level is 0.01° .

In Fig. 3, we show a typical result of a magneto-optical measurement of the perpendicular component of the magnetic field due to superconducting currents in a 100-nm-thick $\text{YBa}_2\text{Cu}_3\text{O}_7$ superconducting ring of 3 mm outer diameter and 125 μm width. The sample was cooled down in zero field. The images were taken at 4.2 K in zero field after a field excursion to 50 mT. The exposure time is 50 ms. In Fig. 3(b), we show the result of the conventional magneto-optic technique³ with rather poor homogeneity of the illumination, while in Fig. 3(c) the ϕ output of the new polarimeter is presented under the same physical conditions. Comparison of Figs. 3(b) and 3(c) clearly shows that: (i) The low contrast in the conventional image is mainly due to uneven illumination, while this nuisance is completely eliminated by the new method. (ii) The sign of the magnetic field, which is opposite at the inside edge of the ring compared to the outside edge, is directly measured with the new technique, while no difference is seen in the conventional experiment. (iii) The new setup greatly enhances the sensitivity for detail. The horizon-

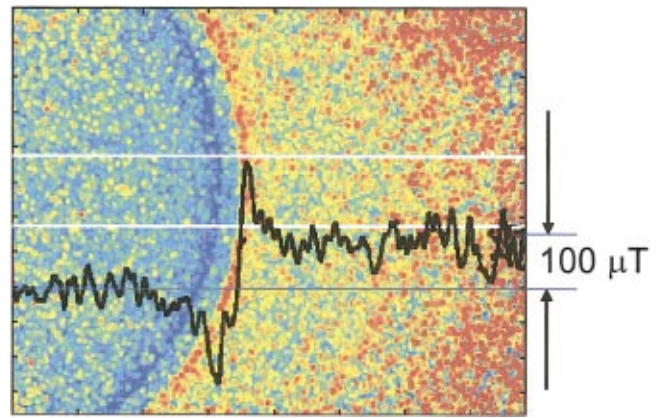


FIG. 4. (Color) Magneto-optical measurement on the same superconducting ring as in Fig. 2, but now in 100 μT external field after zero-field cooling. The effective exposure time is 60 s. The black curve shows an average profile of the region between the white lines. Note that the root-mean-square noise level in the profile is $\sim 10 \mu\text{T}$.

tal and arrow-shaped lines close to the inner edge of the ring are, in fact, modulations due to the presence of domains in the yttrium-iron-garnet (YIG) indicator film.⁶ Note that the profile in Fig. 3(b) contains very little information on the ring itself, in contrast to the profile in Fig. 3(c), which exhibits all the characteristic features of the magnetic field expected for such a ring.⁷

To demonstrate the sensitivity for small magnetic fields, we show in Fig. 4 an image taken at 4.2 K and 100 μT external field after zero-field cooling. The effective exposure time is 60 s. From the profile we find that the root-mean-square (rms) noise level is below 10 μT , corresponding to 4×10^{-4} deg rotation angle. Note that the weaker illumination at the right-hand side only shows up as an increased noise contribution. The typical rms noise level for a single pixel is $0.7 \text{ mT Hz}^{-1/2}$ or $0.03 \text{ deg Hz}^{-1/2}$.

To demonstrate the linearity of the instrument, we show in Fig. 5 a plot of the measured ϕ -output signal (averaged over a 10×10 pixels square) far away from the ring versus external field. At this position ϕ essentially measures the

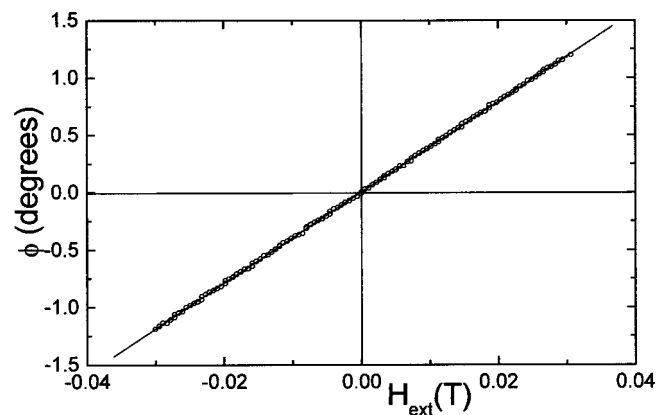


FIG. 5. Measured ϕ -output signal, i.e., polarization rotation, averaged over a 10×10 pixel square far away from the superconducting ring vs external field $\mu_0 H_{\text{ext}}$. At this position ϕ is essentially determined by the external field only. Note that the ϕ output is linear in H_{ext} due to the intrinsic linearity of the new method. The absolute value of ϕ is determined using the calibration of the polarization rotator in a separate experiment.

external field only. Note that this remarkable linear behavior is not due to a linearization procedure, but to the fact that the measurement is inherently linear in field. The scale along the vertical axis is based on a separate calibration of the polarization rotator (PR in Fig. 1).

In conclusion, our new setup is a highly sensitive imaging polarimeter, which has superior sensitivity at small rotation angles and yields directly the rotation angle and its sign. With a slightly more elaborate modulation scheme, incorporating modulation steps with circularly polarized light, our setup can even be adapted to measure the full Mueller⁸ matrix in imaging mode. By placing the modulation optics in front of the camera, it can also be used for remote sensing, e.g., to study far-away light sources in astrophysics (in solar, planetary,⁹ and stellar observations).

ACKNOWLEDGMENTS

The authors thank Dr. B. Dam and J. M. Huijbregtse for providing the superconducting thin film. This work is part of

the research program of the Stichting Fundamenteel Onderzoek der Materie (FOM), which is financially supported by the Nederlandse Organisatie voor Wetenschappelijk Onderzoek (NWO).

¹J. Tinbergen, *Astronomical Polarimetry* (Cambridge University, Cambridge, UK, 1996), see, in particular, Chap. 3.

²See, e.g., D. Clarke and V. Ameijena, *Astron. Astrophys.* **355**, 1138 (2000).

³M. R. Koblichka and R. J. Wijngaarden, *Supercond. Sci. Technol.* **8**, 199 (1995).

⁴H. Nyquist, *Trans. Am. Inst. Electr. Eng.* **47**, 617 (1928).

⁵The SF-59 glass is made by the Schott glass company in Germany.

⁶L. A. Dorosinskii, M. V. Indenbom, V. I. Nikitenko, Y. A. Ossip'yan, A. A. Polyanskii, and V. K. Vlasko-Vlasov, *Physica C* **203**, 149 (1992).

⁷E. H. Brandt, *Rep. Prog. Phys.* **58**, 1465 (1995).

⁸S. Huard, *Polarization of Light* (Wiley, Chichester, 1997).

⁹J. E. Hansen and J. W. Hovenier, *J. Atmos. Sci.* **31**, 1137 (1974).